Electronic Supplementary Information (ESI)

Oxygen hole states facilitated cleavage of Ni-O bonds in the rock-salt phase of conversion-type anode

Shengnan Sun,[‡*a] Jun Zhou,[‡a,b] Debbie Hwee Leng Seng,[a] Hui Ru Tan,[a] Shibo Xi,[c] Xiping Ni,[a] Fengxia Wei,[a] Poh Chong Lim,[a] Ming Lin,[a] Yi Ren,[a] Shijie Wang[*a,b] and Zhi Wei Seh[*a]

[a]Institute of Materials Research and Engineering (IMRE), Agency for Science, Technology and Research (A*STAR), 2 Fusionopolis Way, Innovis #08-03, Singapore 138634, Republic of Singapore.

[b]Future Energy Acceleration & Translation (FEAT), Strategic Research & Translational Thrust (SRTT), Agency for Science, Technology and Research (A*STAR), 2 Fusionopolis Way, Innovis #08-03, Singapore 138634, Republic of Singapore.

[c]Institute of Sustainability for Chemicals, Energy and Environment (ISCE2), Agency for Science, Technology and Research (A*STAR), 1 Pesek Road, Jurong Island, Singapore 627833, Republic of Singapore.

[‡]S.S. and J.Z. contributed equally to this work.

*Corresponding author E-mail:

sun_shengnan@imre.a-star.edu.sg; sj-wang@imre.a-star.edu.sg; sehzw@imre.a-star.edu.sg

Experimental

Material synthesis

The NiO and Li-doped NiO were synthesized with sol-gel method by using lithium nitrate, nickel nitrate hexahydrate, citric acid and urea. These chemicals were purchased from Sigma-Aldrich. The mole ratio of total metal, citric acid and urea were 1/2/2. The feeding mole ratios of Li to Ni were controlled at 0/1, 0.10/0.90, 0.25/0.75 and 0.40/0.60. All these chemicals were dissolved in de-ionized water under constant stirring, and the solution was heated to ~95 °C and kept until the gel formed. Then the gel was transferred to oven (170 °C) and dried overnight. The dried resin was annealed at 1000 °C for 6 h at a ramping rate of 5 °C min^{-1} under flowing air using tube furnace and cooled down naturally. For the synthesis of $Mg_{0.05}Ni_{0.95}O$ and $Mg_{0.50}Ni_{0.50}O$, magnesium nitrate hexahydrate was used as the precursor. For NiO synthesis, a few metallic nickel particles exist in the annealed powders. A magnet was used to remove the metallic nickel particles and, the remaining powders were annealed at 1000 °C for 2 h following the above procedure and collected. All the collected powders were ball-milled for 90 min using agate jar and ball for the material and electrochemical characterization.

Material characterization

Agilent 720ES was used to measure the Li concentration in these synthesized Li-doped NiO powders by the inductively coupled plasma (ICP) method. Bruker D8 Advance Powder X-Ray Diffractometer with Cu-Kα radiation was used to characterize the crystal structure. The X-ray absorption near edge structure (XANES) was studied at the Singapore Synchrotron Light Source, XAFCA beamline.[1] FEI Titan TEM was used to collect the electron energy loss spectroscopy (EELS). Kratos AXIS Supra$^+$ spectrometer with monochromatic Al Kα excitation source (hv=1486.7 eV) was used for X-ray photoelectron spectroscopy (XPS) to detect the surface electronic states of these powders under low energy neutralisation electrons charge compensation, and the adventitious C 1*s* at 284.8 eV was used for charge shift correction. The Li 1*s* and Ni $2p_{3/2}$ spectra were also used for the quantification of the Li concentration in the synthesized oxides. The Micromeritics® ASAP® 2460 Surface Area and Porosimetry Analyzer was used to evaluate the surface areas of those synthesized powders.

Electrochemical test

The oxide electrodes were prepared by casting a slurry containing 80 wt% oxide, 10 wt% carbon black (Super P® Conductive, 99+%, Alfa Aesar) and 10 wt% poly(vinylidene fluoride) (PVDF, average Mw ~534,000 by GPC, Sigma-Aldrich) (in 1-Methyl-2-pyrrolidinone, ACS reagent, ≥99.0%, Sigma-Aldrich) onto the Cu foil (~10 μm). The poly(vinylidene fluoride) powders were dissolved into 1-Methyl-2-pyrrolidinone (NMP, ACS reagent, ≥99.0%, Sigma-Aldrich) to form 5 wt% PVDF solution. The coatings were dried in the vacuum oven at 80 °C overnight. The electrodes were cut into 1 cm^2 disks (diameter 11.28 mm). The typical oxide mass loading is 1-2 mg cm^{-2}. Coin-type cells (CR2032) with lithium chip (12.5 mm × 0.5 mm) and glass microfiber filters (diameter 16.2 mm, Whatman GF/A CAT No.1820-915) as separator using the electrolyte 1.0 M $LiPF_6$ in ethylene carbonate (EC) and diethyl carbonate (DEC), EC/DEC = 50/50 (v/v, CANRD). The coin cells were assembled inside the argon-filled glovebox ([Oxygen] < 0.1 ppm, [Moisture] < 0.5 ppm). The charge-discharge curves and galvanostatic intermittent titration technique (GITT) were tested by NEWARE Battery Testing System. The cyclic voltammetry

(CV) curves were tested by Gamry Instrument Interface 1010E and Reference 3000 potentiostats. All coin cells were under static stabilization over 24 hours before electrochemical tests.

Calculation methods

The density functional theory (DFT) simulations are performed by the Vienna ab initio Simulation Package (VASP 5.4.4).[2,3] The Perdew-Burke-Ernzerhof (PBE) approximation is utilized for the exchange-correlation functional, and the frozen-core all-electron projector augmented wave (PAW) method is employed to describe the electron-ion interaction.[4] The cutoff energy for the plane wave expansion is set to 500 eV. For bulk NiO, an antiferromagnetic configuration with 64 atoms is used. For all simulations, k-point grids of Monkhorst-pack 6×6×6 and 6×6×1 are applied for the bulks and surface slab models, respectively. The generalized gradient approximation (GGA) with Hubbard U of 5 eV is used specifically for the *d* orbitals of Ni.[5,6] The atoms within the structure are fully relaxed until both the energy and force converge to 10^{-5} eV and 0.01 eV/Å, respectively.

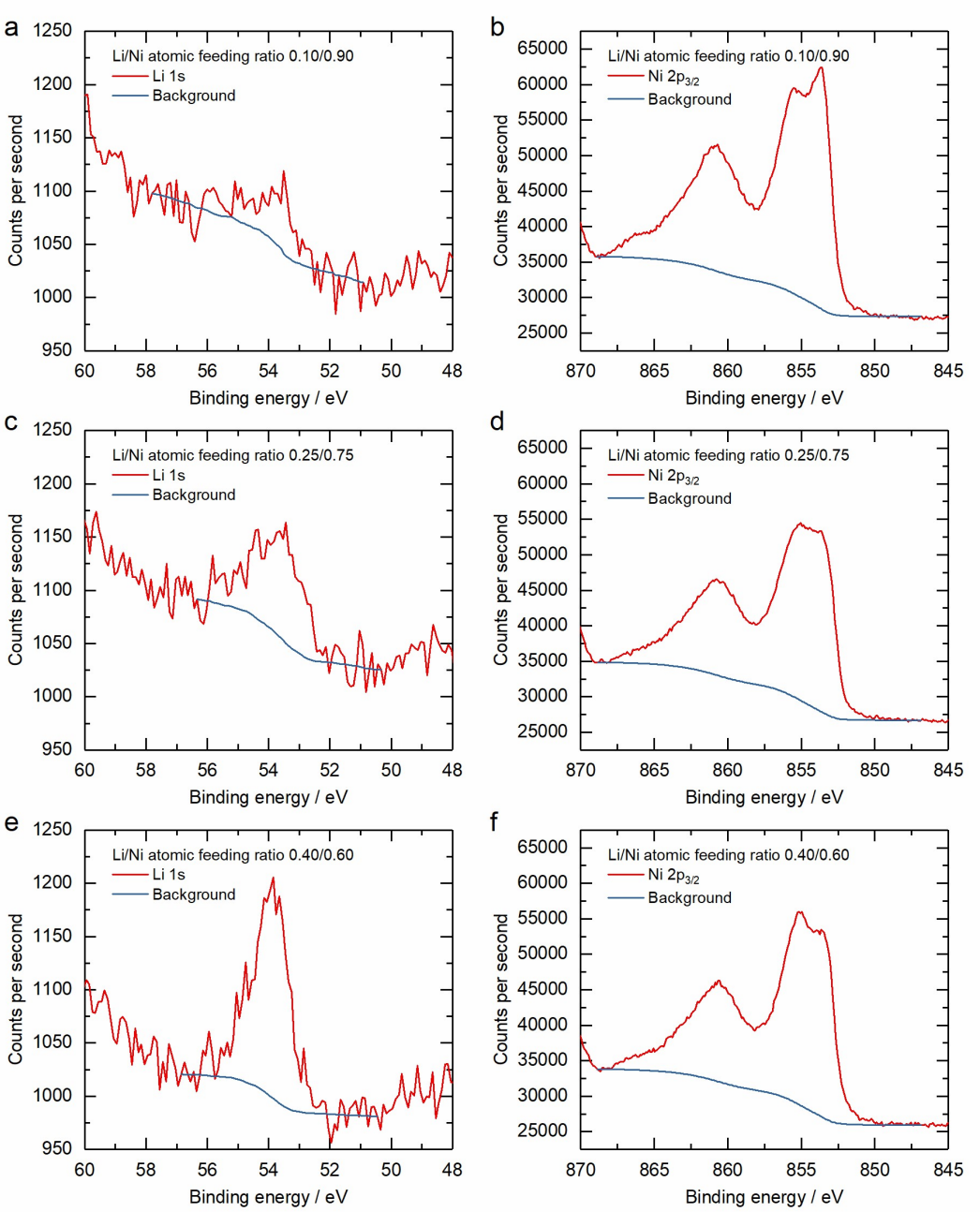

Fig. S1. The raw XPS spectra for the quantification of Li and Ni atomic concentrations in these synthesized oxides. For Li/Ni atomic feeding ratio 0.10/0.90, (a) Li 1s and (b) Ni $2p_{3/2}$. For Li/Ni atomic feeding ratio 0.25/0.75, (c) Li 1s and (d) Ni $2p_{3/2}$. For Li/Ni atomic feeding ratio 0.40/0.60, (e) Li 1s and (f) Ni $2p_{3/2}$.

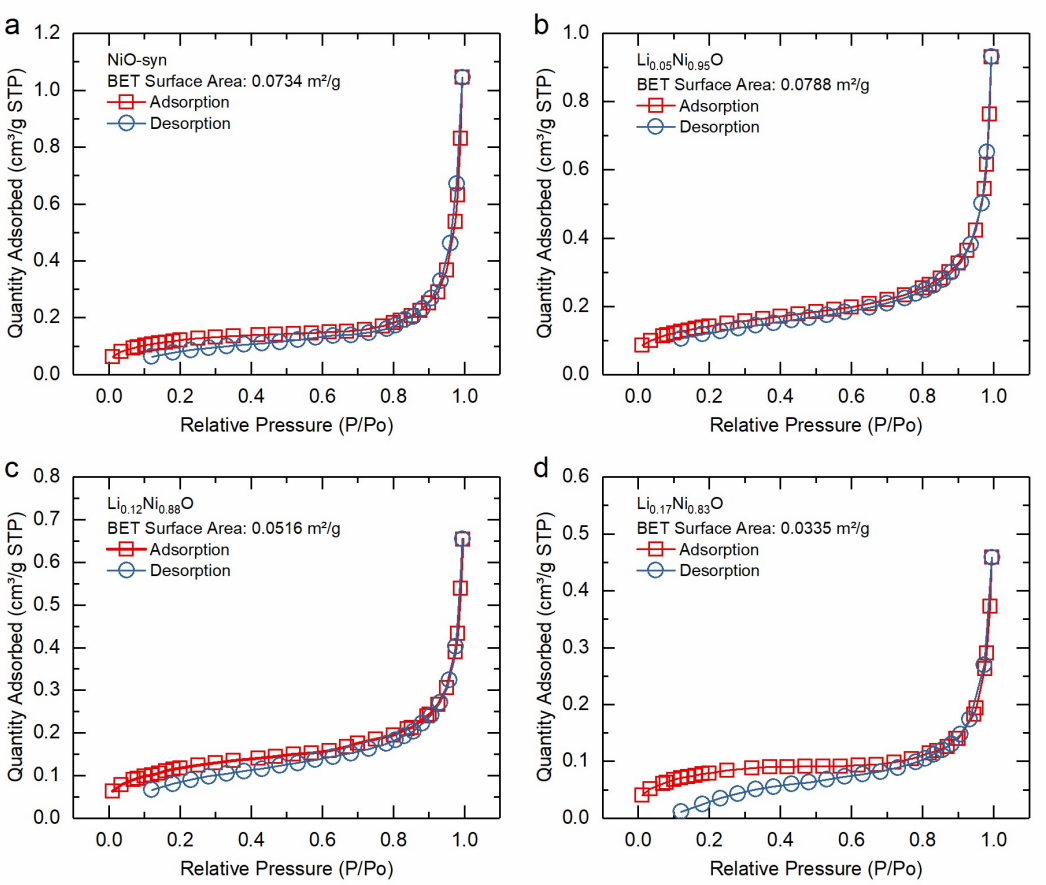

Fig. S2. The adsorption-desorption isotherms of (a) NiO-syn, (b) $Li_{0.05}Ni_{0.95}O$, (c) $Li_{0.12}Ni_{0.88}O$, and (d) $Li_{0.17}Ni_{0.83}O$ for the surface area. Analysis adsorptive: N_2. Analysis bath temperature: -195.800 °C. The Brunauer-Emmett-Teller (BET) surface areas are shown in each sub-figure.

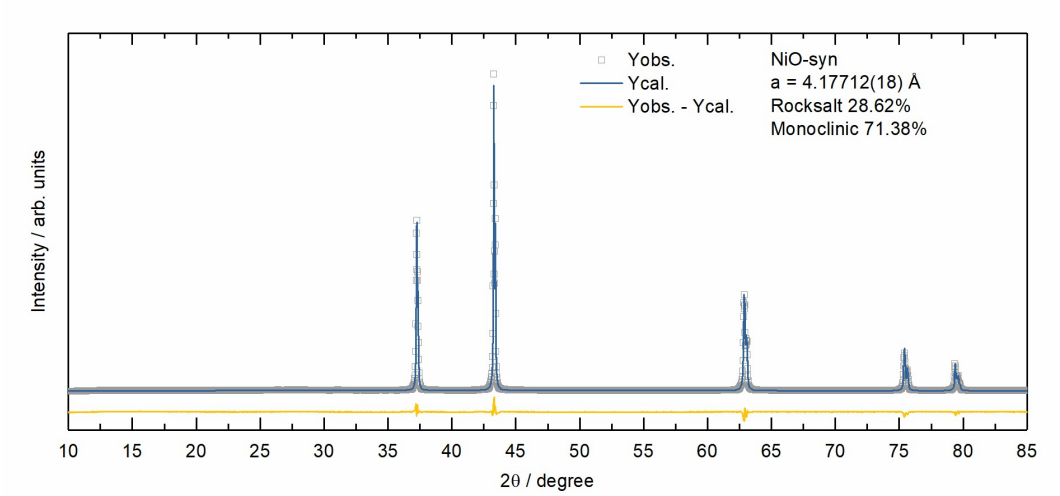

Fig. S3. XRD Rietveld refinement of NiO-syn.

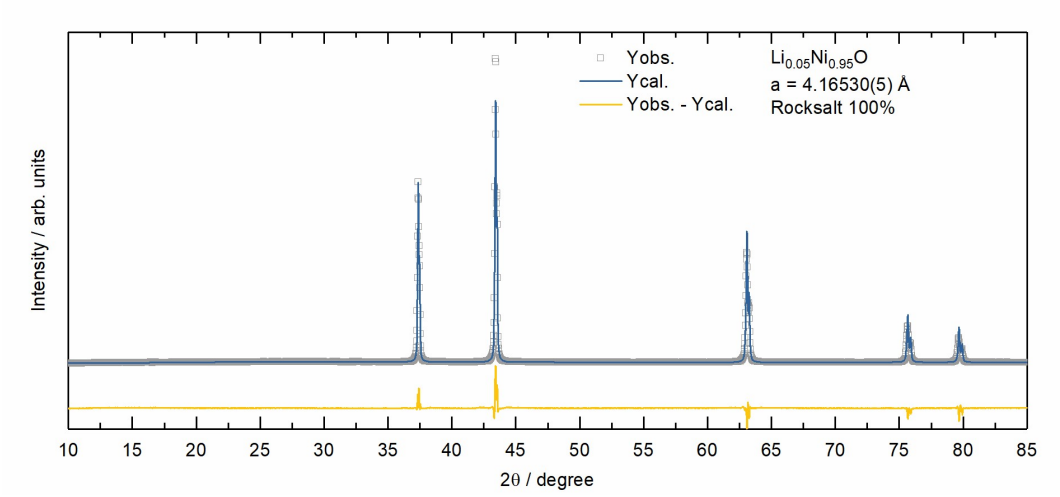

Fig. S4. XRD Rietveld refinement of synthesized $Li_{0.05}Ni_{0.95}O$.

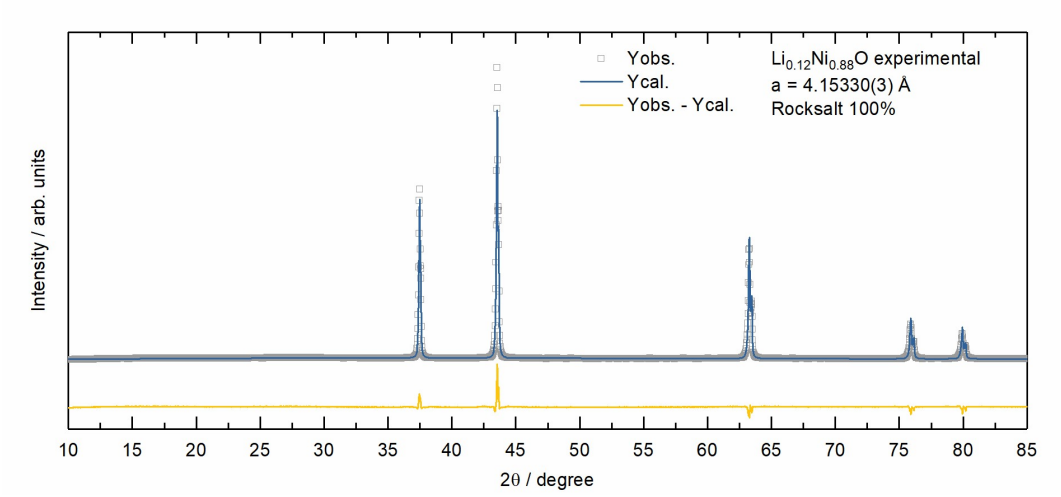

Fig. S5. XRD Rietveld refinement of synthesized $Li_{0.12}Ni_{0.88}O$.

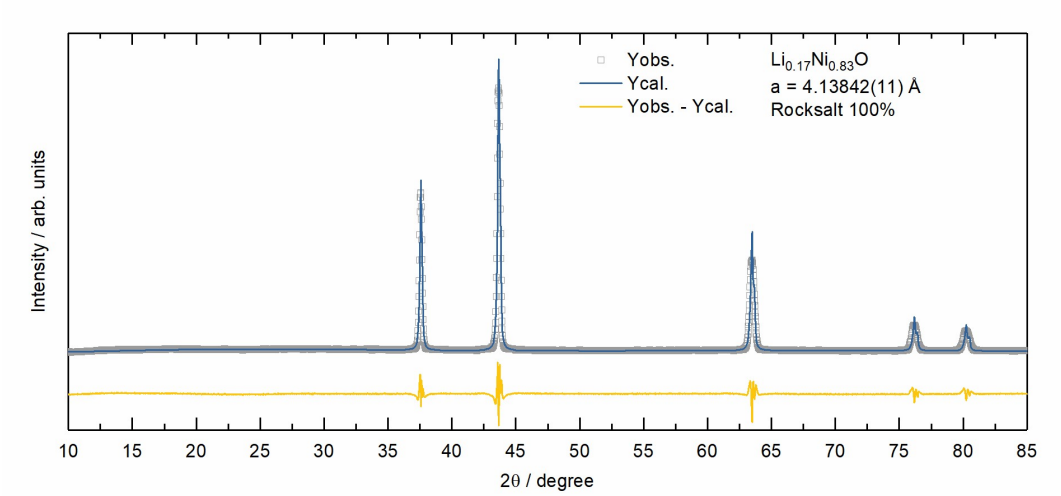

Fig. S6. XRD Rietveld refinement of synthesized $Li_{0.17}Ni_{0.83}O$.

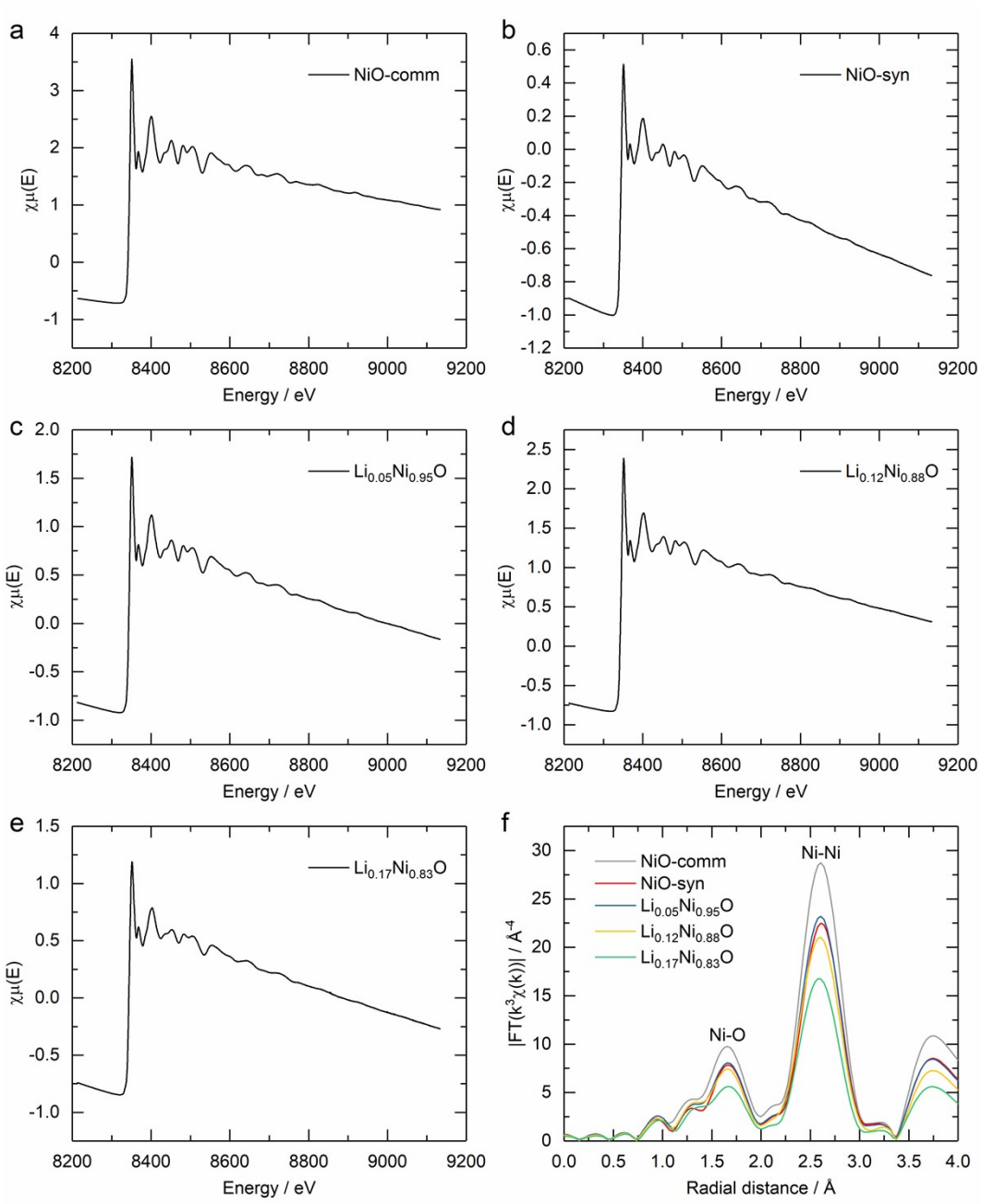

Fig. S7. The EXAFS experimental data of Ni K-edges of (a) the commercial NiO, (b) the synthesized NiO, (c) $Li_{0.05}Ni_{0.95}O$, (d) $Li_{0.12}Ni_{0.88}O$ and (e) $Li_{0.17}Ni_{0.83}O$, and (f) their k^3-weighting FT-EXAFS.

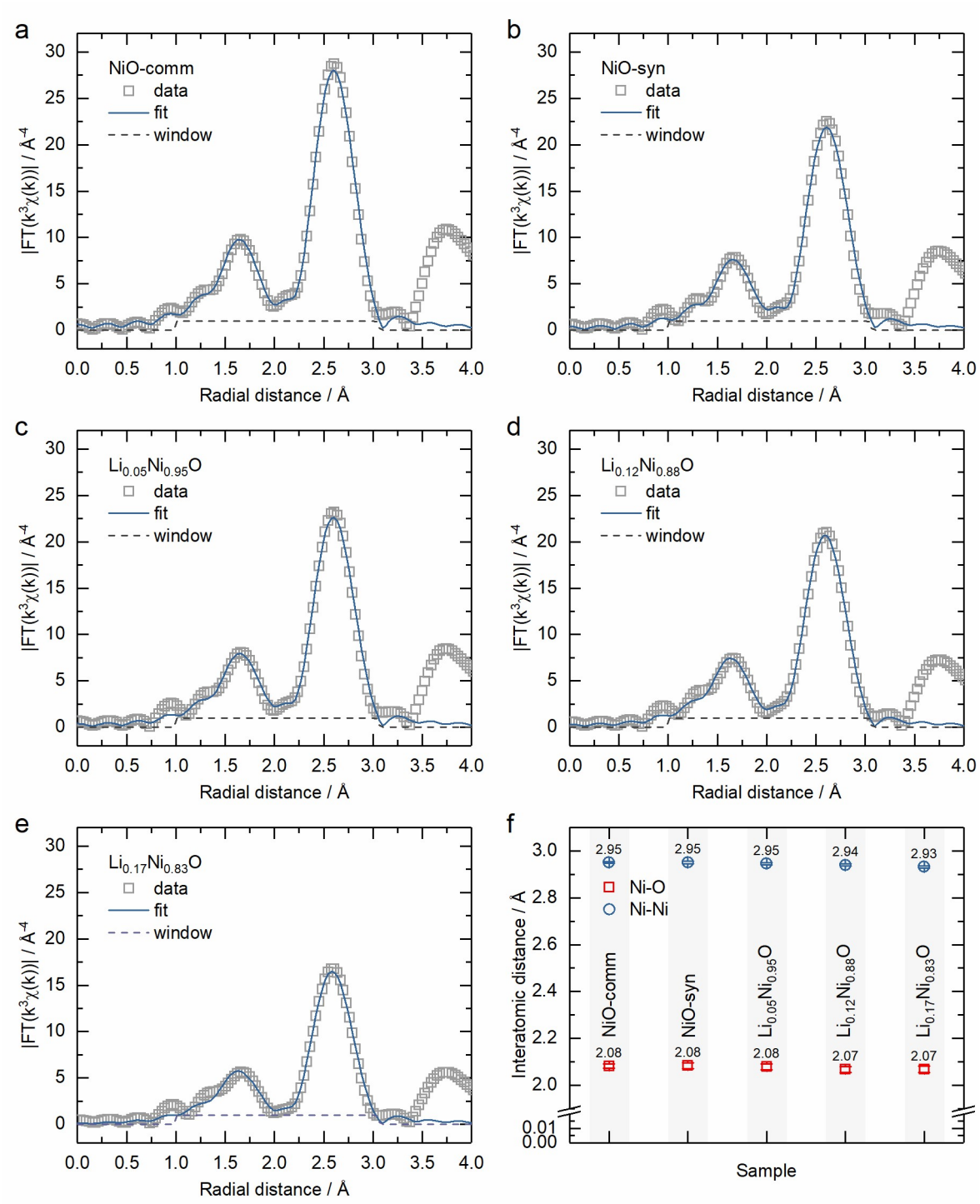

Fig. S8. The k^3-weighting FT-EXAFS and the fitting of (a) the commercial NiO, (b) the synthesized NiO, (c) $Li_{0.05}Ni_{0.95}O$, (d) $Li_{0.12}Ni_{0.88}O$ and (e) $Li_{0.17}Ni_{0.83}O$ of Ni K-edges under a Hanning-shaped window, fixing the coordination number to 6 for the first shell and 12 for the second shell for the commercial NiO, and (f) the fitted interatomic distance of Ni-O in the first shell and Ni-Ni in the second shell.

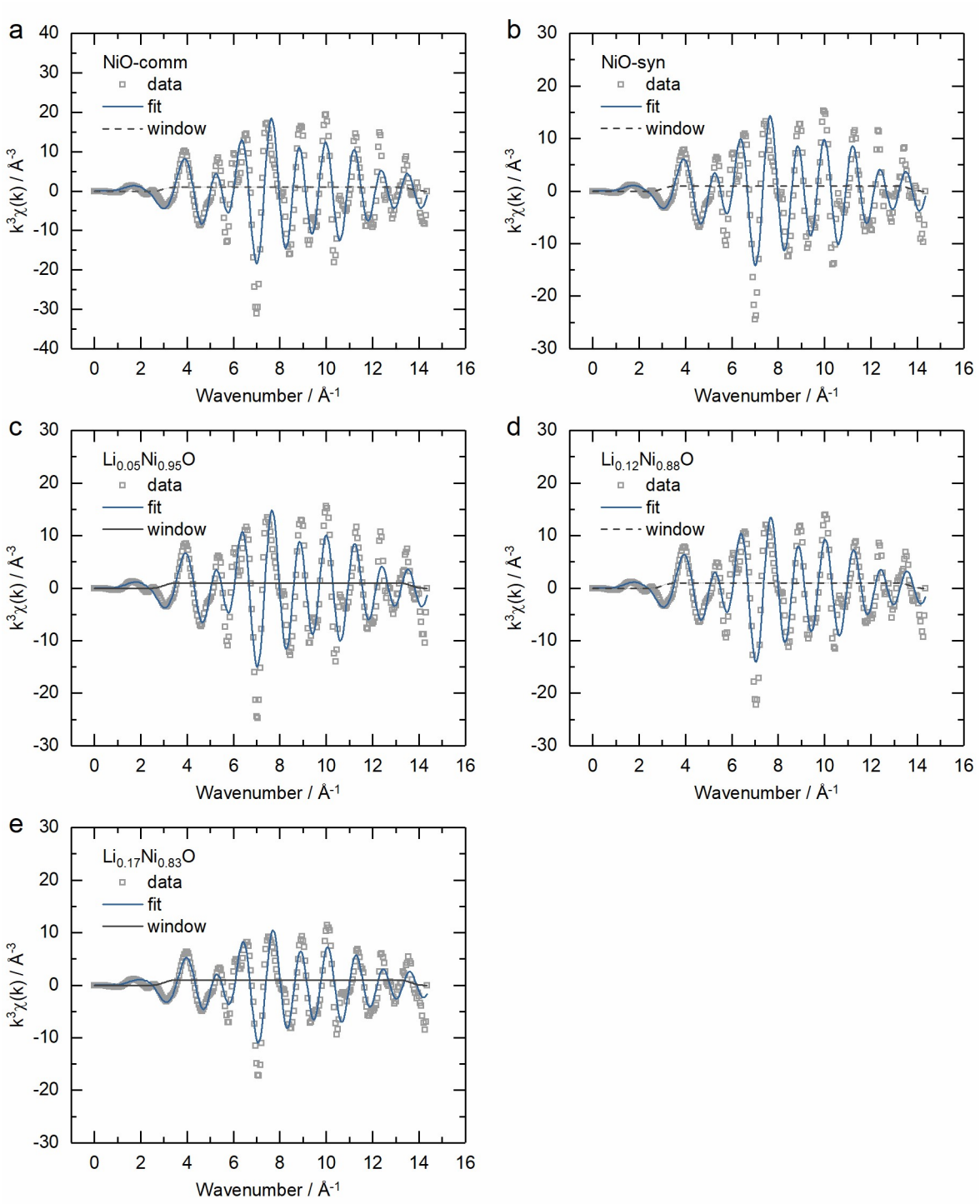

Fig. S9. The fitted EXAFS results of (a) the commercial NiO, (b) the synthesized NiO, (c) $Li_{0.05}Ni_{0.95}O$, (d) $Li_{0.12}Ni_{0.88}O$ and (e) $Li_{0.17}Ni_{0.83}O$ of Ni K-edges in k-space under a Hanning-shaped window.

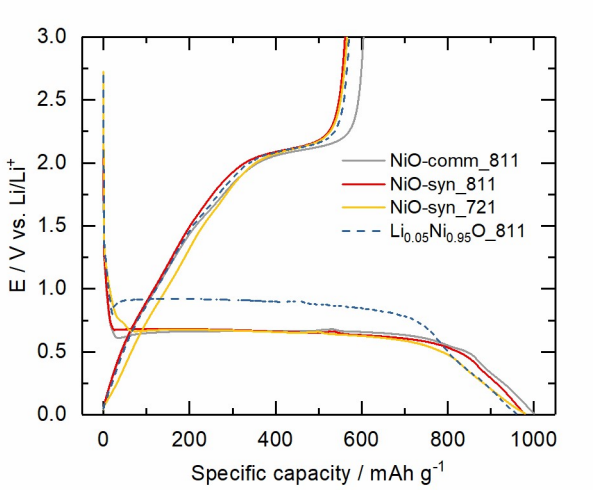

Fig. S10. The first lithiation and de-lithiation curves of the synthesized NiO composite electrode with the oxide/carbon black/binder mass ratios 8/1/1 (NiO-syn_811) and 7/2/1 (NiO-syn_721), and the commercial NiO with the oxide/black/binder mass ratios 8/1/1 (NiO-comm_811). The data of $Li_{0.05}Ni_{0.95}O$ composite electrode with the oxide/carbon black/binder mass ratios 8/1/1 ($Li_{0.05}Ni_{0.95}O$_811) are also included for reference.

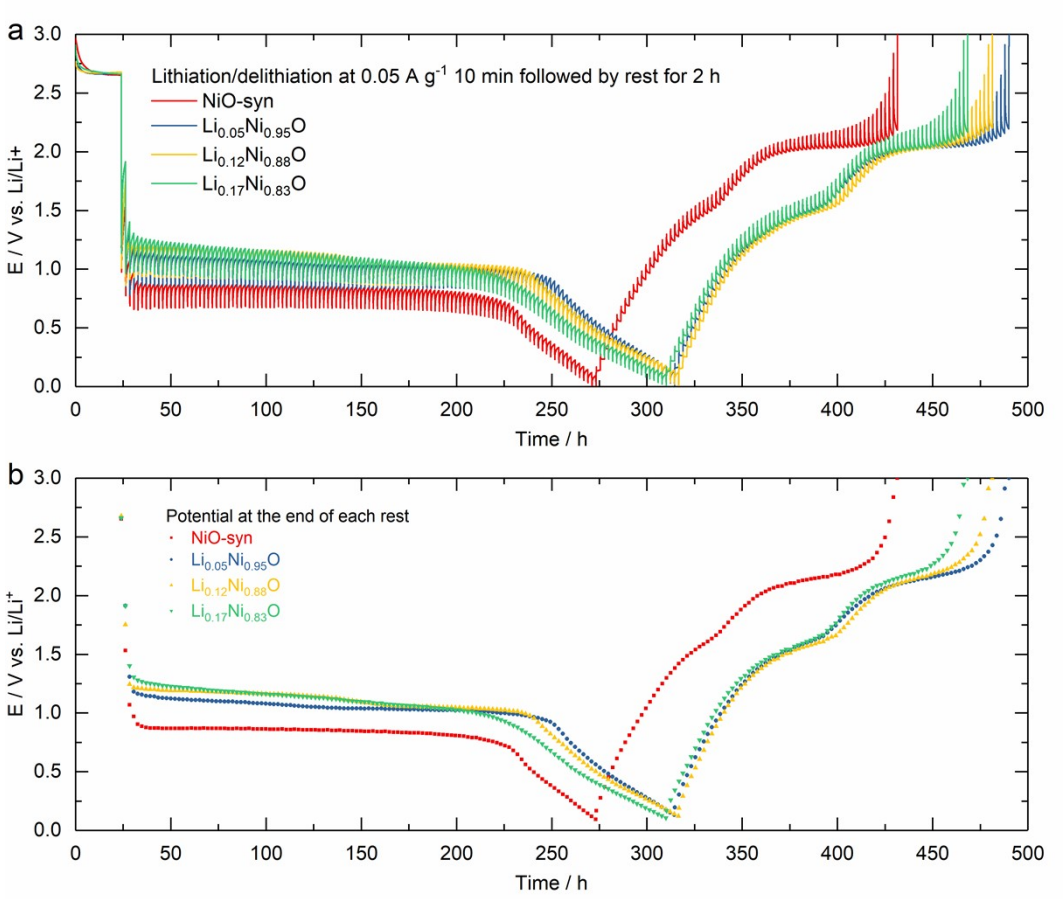

Fig. S11. (a) GITT tests and (b) the potential at the last second of each rest period in GITT tests of the synthesized NiO and Li-doped NiO at a current density of 0.05 A g^{-1} lithiation/delithiation followed by resting for 2 hours.

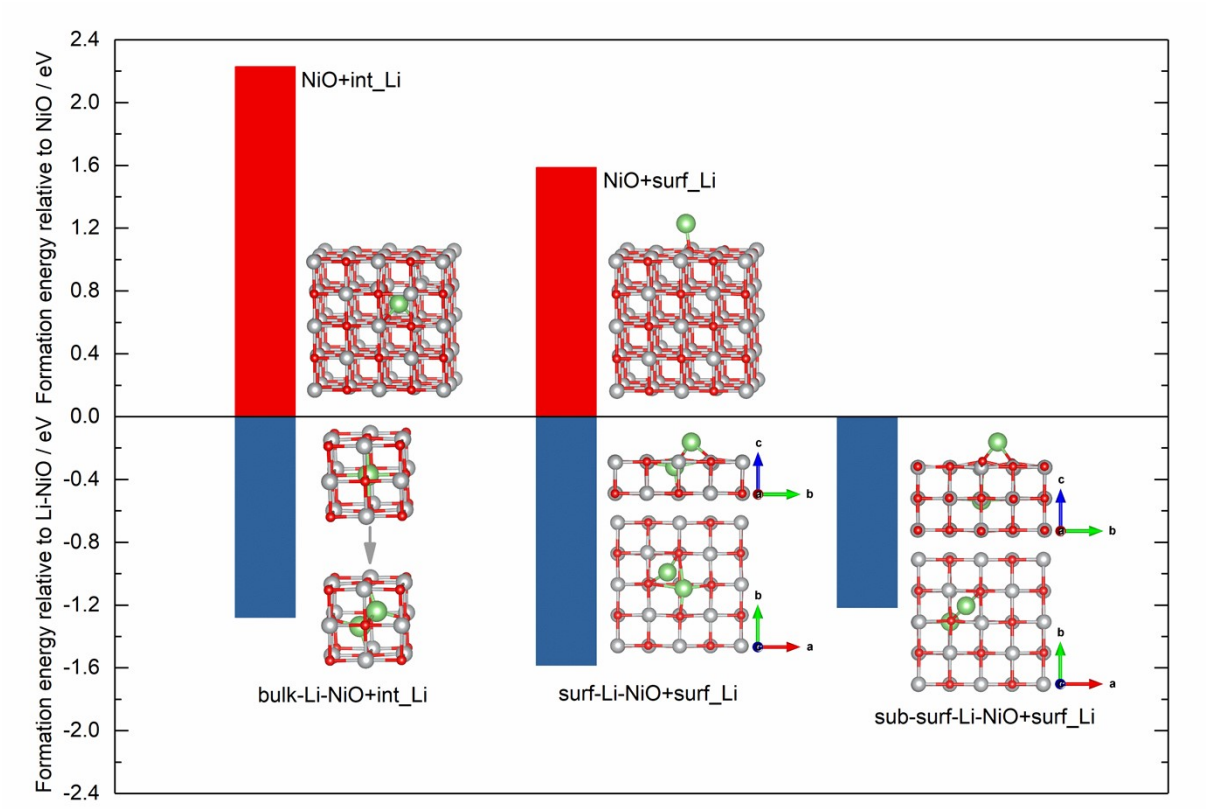

Fig. S12. The formation energy of inserting one interstitial Li (int_Li) into NiO bulk and adding one surface Li (surf_Li) onto NiO surface, and inserting one int_Li into Li-doped NiO (Li-NiO), adding one surf_Li onto the surface Li doped NiO (surf-Li-NiO) and sub-surface Li doped NiO (sub-surf-Li-NiO). The green, grey and red balls represent the lithium, nickel and oxygen atoms, respectively.

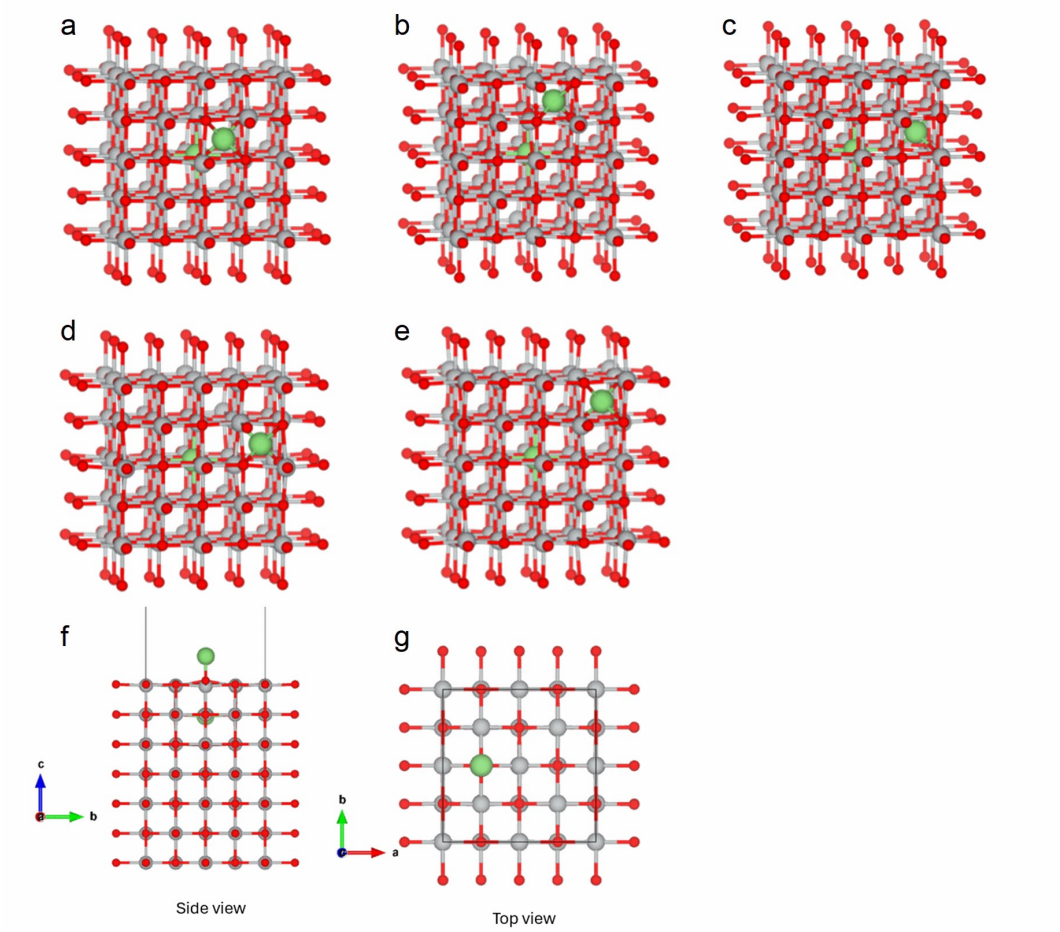

Fig. S13. The other configurations for inserting one interstitial Li into the Li-doped NiO (upper panel). Their formation energies are (a) 1.06, (b) 0.92, (c) 1.55. (d) 0.92 and (e) 0.99 eV higher than the ground-state configuration. The other configuration of adding one Li onto the surface of Li-doped NiO (lower panel, f and g). The formation of this surface Li is 1.17 eV and thus will be unlikely to form. The green, grey and red balls represent the lithium, nickel and oxygen atoms, respectively.

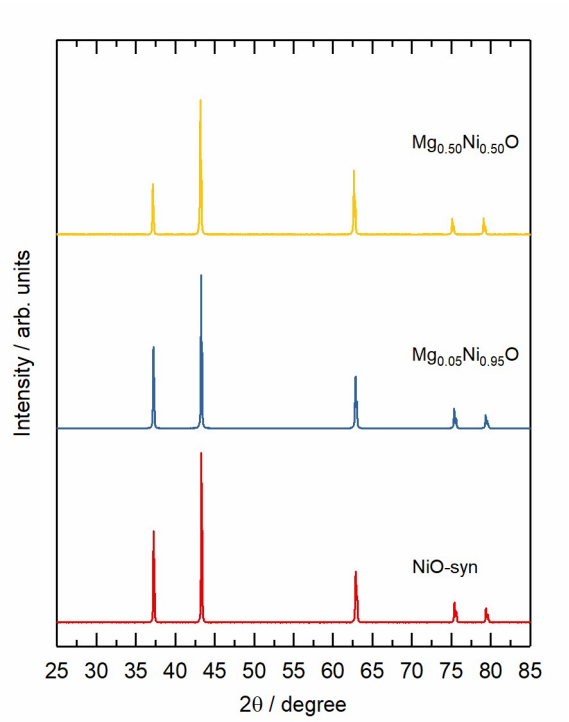

Fig. S14. XRD patterns of NiO-syn, $Mg_{0.05}Ni_{0.95}O$ and $Mg_{0.50}Ni_{0.50}O$.

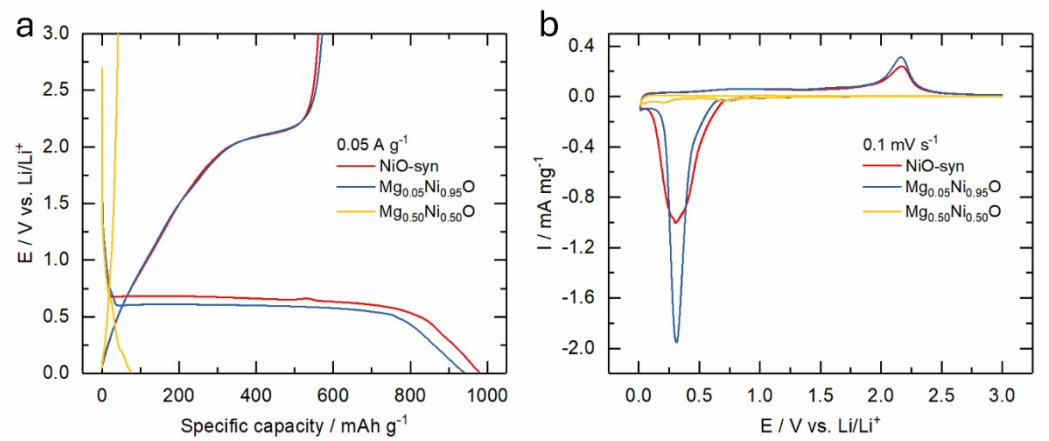

Fig. S15. The comparison of synthesized NiO and $Mg_{0.05}Ni_{0.95}O$ and $Mg_{0.50}Ni_{0.50}O$ with the oxide/carbon black/binder mass ratios 8/1/1. (a) The first lithiation and de-lithiation and (b) CV curves.

Table S1. The Li/Ni atomic ratios of feeding in synthesis and oxide powders obtained from ICP and XPS tests.

Li/Ni atomic feeding ratio	Li/Ni atomic ratio in oxide powders from ICP	Li/Ni atomic ratio in oxide powders from XPS
0.10/0.90	0.046/0.954	0.050/0.950
0.25/0.75	0.117/0.883	0.113/0.887
0.40/0.60	0.175/0.825	0.156/0.844

Table S2. EXAFS fitting parameters of NiO and Li-doped NiO

Edge	Path	CN	σ^2 / Å^2	ΔE_0 / eV	R / Å	R-factor
NiO-comm	Ni-O	6	0.0058(0.0008)	0.48(1.57)	2.08(0.01)	0.004
	Ni-Ni	12	0.0062(0.0004)	-0.96(0.71)	2.95(0.00)	
NiO-syn	Ni-O	4.1(0.7)	0.0047(0.0014)	1.61(2.20)	2.08(0.01)	0.006
	Ni-Ni	8.9(0.8)	0.0059(0.0005)	-0.03(0.97)	2.95(0.00)	
$Li_{0.05}Ni_{0.95}O$	Ni-O	4.6 (0.8)	0.0054(0.0015)	1.53(2.15)	2.08(0.01)	0.006
	Ni-Ni	9.7(0.9)	0.0062(0.0005)	-0.57(0.96)	2.95(0.00)	
$Li_{0.12}Ni_{0.88}O$	Ni-O	4.5(0.7)	0.0059(0.0014)	1.18(2.05)	2.07(0.01)	0.005
	Ni-Ni	9.2(0.8)	0.0064 (0.0005)	-0.64(0.91)	2.94(0.00)	
$Li_{0.17}Ni_{0.83}O$	Ni-O	3.7 (0.7)	0.0068(0.0017)	2.79(2.25)	2.07(0.01)	0.007
	Ni-Ni	7.0(0.7)	0.0062 (0.0006)	-0.59(1.02)	2.93(0.01)	

Note: CN, coordination number; σ^2, Debye-Waller factor to account for both thermal and structure disorder; ΔE_0, inner potential correction; R, distance between absorber and backscatter atoms; R-factor indicates the goodness to the fit. The amplitude reduction factor S_0^2 was fixed to 0.916 for Ni. Fitting range: Ni K-edge $3.0 \leq k$ (/Å) ≤ 13.654 and $1.0 \leq R$ (Å) ≤ 3.05.

Author contributions

S.S. and J.Z. contributed equally to this work. S.S. conceived the original concept, initiated the project and wrote the manuscript. J.Z., S.W. and Z.W.S. revised it. S.S. synthesized the materials and performed the characterization with assistance from D.H.L.S. (XPS), H.R.T. (EELS), S.X. (XANES), X.N. (BET), F. W. (XRD Rietveld refinement), and P.C.L. (XRD). M.L. and Y.R. joined the discussion and analysis on EELS and XPS, respectively. J.Z. carried out the theoretical calculation and results analysis. S.W. supervised and financially support the simulation work. Z.W.S. supervised and financially support the experimental work.

References

1 Y. Du, Y. Zhu, S. Xi, P. Yang, H.O. Moser, M.B.H. Breese and A. Borgna, *J. Synchrotron Radiat.*, 2015, **22**, 839-843.

2 G. Kresse and J. Hafner, *Phys. Rev. B*, 1993, **47**, 558-561.

3 G. Kresse and J. Hafner, *Phys. Rev. B*, 1994, **49**, 14251-14269.

4 G. Kresse and D. Joubert, *Phys. Rev. B*, 1999, **59**,1758-1775.

5 J. Hubbard, *Proc. R. Soc. Lond. A*, 1963, **276**, 238-257.

6 S.L. Dudarev, G.A. Botton, S.Y. Savrasov, C.J. Humphreys and A.P. Sutton, *Phys. Rev. B*, 1998, **57**, 1505-1509.